Angewandte Chemie
Eine Zeitschrift der Gesellschaft Deutscher Chemiker

Supporting Information

69451 Weinheim, Germany

Characterizing Methyl-Bearing Side Chain Contacts and Dynamics Mediating Amyloid β Protofibril Interactions Using $^{13}C_{methyl}$-DEST and Lifetime Line Broadening**

Nicolas L. Fawzi, David S. Libich, Jinfa Ying, Vitali Tugarinov, and G. Marius Clore**

anie_201405180_sm_miscellaneous_information.pdf

Supporting Information

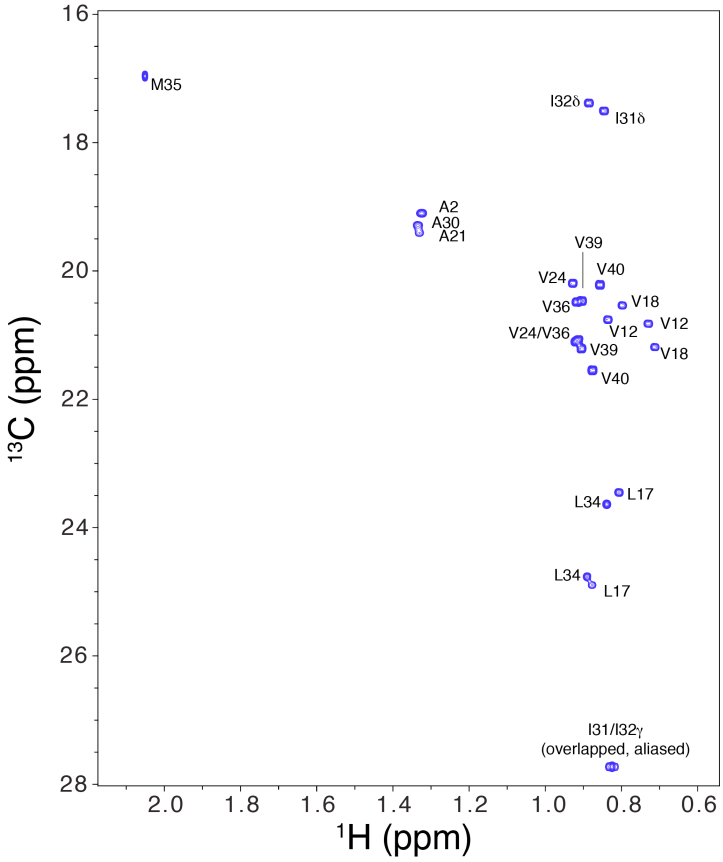

Figure S1 . ^{1}H-^{13}C constant-time HSQC spectrum of U-[^{13}C,^{15}N] labeled Aβ40. The constant time period is 54 ms. Assignment of the resolved methyl groups of monomeric Aβ40 was initially achieved using the U-[^{13}C/^{15}N] sample by directly correlating ^{1}H methyl resonances with the previously assigned backbone $^{1}H_N$/^{15}N resonances[S1] in a 3D ^{15}N-separated ^{1}H-^{1}H TOCSY spectrum recorded with high resolution at 600 MHz in the indirect ^{1}H dimension achieved by selectively exciting methyl protons with 4ms EBURP2/time-reversed EBURP2 pulses centered at 0.3 ppm prior to ^{1}H isotropic mixing. The ^{13}C methyl resonances were then identified from the ^{1}H-^{13}C correlations in a 56 ms constant-time HSQC spectrum. The assignment was further confirmed by first correlating the ^{13}C methyl resonances with the well resolved $^{1}H_{\alpha}$/$^{13}C_{\alpha}$ resonances[S2] in a 3D ^{13}C-TOCSY spectrum and then correlating the $^{1}H_{\alpha}$ resonance with the known $^{1}H_N$ chemical shift in a 3D $^{13}C_{\alpha}$-separated ^{1}H-^{1}H TOCSY spectrum using a 100 μM sample of U-[^{13}C] labeled Aβ40.

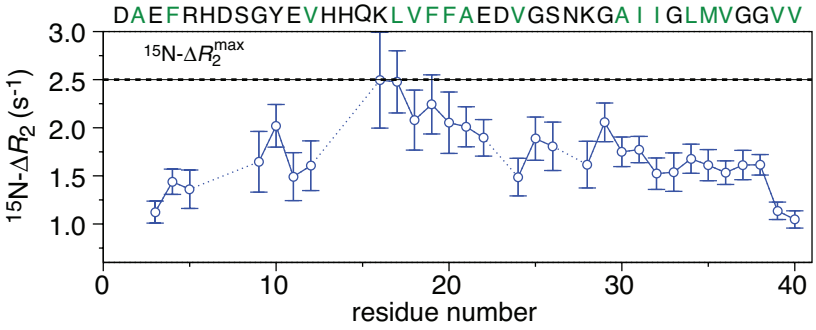

Figure S2. ^{15}N-ΔR_2 values as a function of residue measured from the difference in ^{15}N-R_2 values measured on the same 240 and 50 μM samples (total concentration) of ^{13}C/^{15}N-labeled Aβ40 used for the $^{13}C_{methyl}$ measurements. The amino acid sequence is displayed on top with hydrophobic residues colored in green.

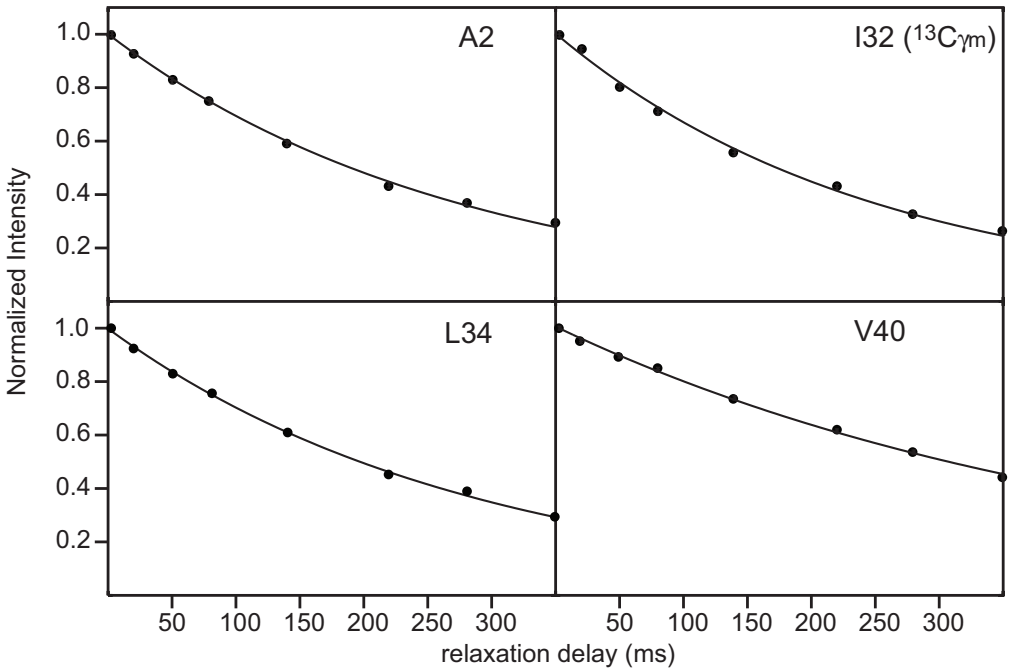

Figure S3. Plots of representative methyl ^{13}C $R_{1\rho}$ relaxation curves for Ala2, Ile32, Leu34 and Val40. No stereo-specific assignments were made for Leu and Val methyl groups. In all cases, the decay curves can be very well fitted to a single exponential, indicating that in this instance the cross-correlated relaxation effect is negligibly small.

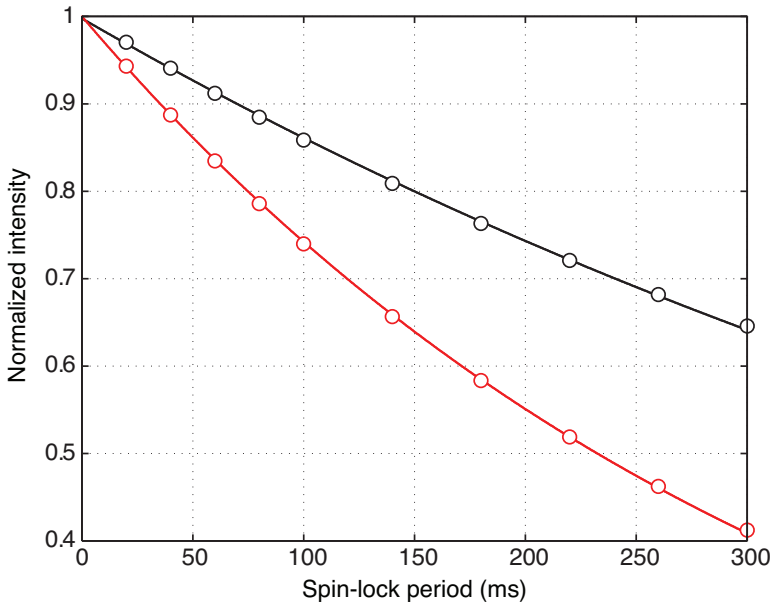

Figure S4. The effects of ^{1}H-^{13}C/^{1}H-^{13}C dipole-dipole cross-correlated relaxation in methyl groups on the accuracy of $^{13}C_{methyl}$-ΔR_2 values are alleviated in this work by the application of 120° ^{1}H pulses[S3] with inter-pulse periods of 30 ms during the spin-lock period of the $R_{1\rho}$ pulse sequence . If the rate of application of these pulses is fast compared to the decay rate of the fast-relaxing components of methyl magnetization, the relaxation rates of the 3/2 spin manifold transitions are effectively averaged leading to a bi-exponential decay of the total methyl magnetization with equal weights (1/2) of the two exponents[S3]. This ensures reliable fitting of relaxation decays to single-exponential functions and extraction of robust lifetime line broadening ($^{13}C_{methyl}$-ΔR_2) contributions. The figure shows simulated relaxation decay curves of methyl ^{13}C magnetization without (black) and with (red) ΔR_2 contributions. In each case, the simulated data-points are fitted to a single-exponential function $Ae^{-R_2 t}$ by optimizing the values of A and R_2, where A is a scale factor, R_2 the relaxation rate, and T the relaxation delay. The difference in the rates obtained from the fits is compared to the ΔR_2 value input *a-priori* into the calculation of the relaxation decay. In the range of relaxation parameters relevant for the present study of Aβ40 aggregation, the errors in estimated ΔR_2 values from ^{1}H-^{13}C/^{1}H-^{13}C dipole-dipole cross-correlated relaxation do not exceed 0.6% - well below the experimental uncertainties in the measurements.

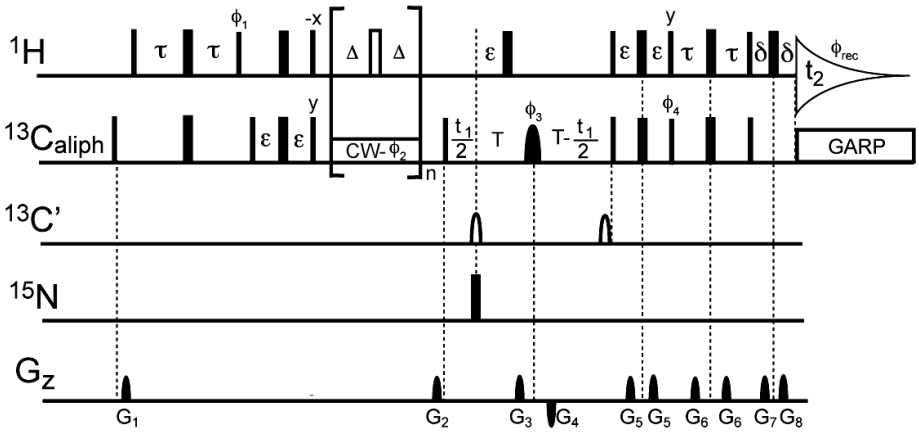

Figure S5. Pulse sequence for the 2D ^{13}C DEST experiment applicable to methyl as well as all other aliphatic groups. Narrow and wide filled-in bars represent 90° and 180° pulses, respectively, and the wide, open bar represents a 120° ^{1}H pulse. The rectangular box ϕ_2 is the low power CW saturation pulse. The filled-in shaped pulse ϕ_3 has a RE-BURP[S4] profile with duration 500 μs (centered at 38 ppm for a ^{13}C frequency of 150.9 MHz). The open shaped pulses are 200 μs 180° sinc (central lobe only) pulses applied at 176 ppm for decoupling ^{13}C' from $^{13}C_\alpha$ and for Bloch-Siegert phase shift compensation. Unless otherwise indicated, all the pulses have phase x; ϕ_1 = y, -y; ϕ_2 = 4(x), 4(-x); ϕ_3 = 2(x), 2(y), 2(-x), 2(-y); ϕ_4 = y; and ϕ_{rec} = x, -x, -x, x. Quadrature detection in the indirect ^{13}C dimension is achieved using an echo-antiecho scheme by inverting the polarity of the G_3 and G_4 gradient pulses and the ^{13}C pulse ϕ_4. The G_1, G_2, G_3, G_4, G_5, G_6, G_7, and G_8 gradient pulses are sine-shaped and have durations of 1.2, 1.1, 0.5, 0.5, 0.47, 1.5, 0.5, and 0.751 ms, respectively. Their corresponding peak powers are 28.7, 25.9, 39.9, -39.9, 11.9, 3.5, 39.9, and 39.9 G/cm along the *z*-axis. Delays: τ = 1.7 ms, ε = 0.86 ms, Δ = 15 ms, δ = 0.86 ms, T = 27.5 ms. For the saturation experiments, a 0.48 s (i.e. n = 16) ^{13}C CW pulse centered at 18 frequencies (-23.7, -20, -16, -10, -8, -6, -4, -2, 0, 2, 4, 6, 8, 10, 16, 20, 23.7, 26 kHz from the carrier at 19 ppm) was applied at two RF field strengths (763 and 1523 Hz). In the two reference experiments, the ^{13}C saturation pulse is turned off while application of the 120° ^{1}H pulse train remains active. The ^{13}C DEST experiment starts with INEPT transfer of ^{1}H magnetization to create antiphase $2C_yH_z$, followed by a refocusing INEPT to rephase $2C_yH_z$ into in-phase C_x, thereby obtaining a C_z term prior to the ^{13}C CW saturation period. It should be noted that for an AX_3 spin system such as the methyl group, it is not possible to completely rephase the anti-phase to the in-phase ^{13}C term, and various terms including $2C_yH_z$, $4C_xH^1{}_zH^2{}_z$, $4C_xH^1{}_zH^3{}_z$, $4C_xH^2{}_zH^3{}_z$, and $8C_yH^1{}_zH^2{}_zH^3{}_z$ remain. The 90° ^{1}H pulse applied at the end of the refocusing INEPT and the subsequent gradient pulse G_2 eliminate $2C_yH_z$ and $8C_yH^1{}_zH^2{}_zH^3{}_z$, but only partially suppress the doubly antiphase terms $4C_xH^1{}_zH^2{}_z$, $4C_xH^1{}_zH^3{}_z$, and $4C_xH^2{}_zH^3{}_z$. As pointed out by Baldwin and Kay,[S5] the generation of these doubly anti-phase terms has a trigonometric dependence of $[1\text{-}3\cos^2(2\pi\ {}^1J_{CH}\ \varepsilon)]$, and therefore these terms can be suppressed by setting the total $^1J_{CH}$ evolution time 2ε such that $1\text{-}3\cos^2(2\pi\ {}^1J_{CH}\ \varepsilon) = 0$. As our work initially aimed to simultaneously measure the DEST effect for all $CH/CH_2/CH_3$ groups in one experiment, a total delay of 1.72 ms was used for 2ε. The effect of residual doubly anti-phase terms on the DEST measurement is expected to be negligibly small, although a pure C_z term prior to DEST saturation helps to minimize, but not completely eliminate, dipole-dipole cross correlated relaxation, an effect that leads to non-exponential decay of ^{13}C-methyl magnetization. The application of the 120° ^{1}H pulse

train at 30 ms intervals during DEST saturation suppresses cross-correlated relaxation between dipolar-CSA interactions.[S3] In addition the 120° ^{1}H pulse train partially mixes the two outer and two inner components of the ^{13}C-methyl quartet,[S6] thereby reducing but not eliminating the dipolar/dipolar relaxation interference effect. After CW saturation, constant-time ^{13}C chemical shift evolution takes place, followed by a Rance-Kay scheme for gradient and sensitivity enhanced detection.

It should be noted that the 120° ^{1}H pulse train does not decouple the methyl protons from the methyl carbons, which in principle may cause the two outermost multiplet components (3 x $^{1}J_{CH}$ = 375 Hz apart) to be saturated at a different level, particularly when the RF power of the saturation pulse is weak. However, the DEST saturation profiles for Aβ40 in the presence and absence of protofibrils are most different at saturation offsets of around 5-8 kHz, a range of resonance offset frequencies that essentially determine the values of the various parameters obtained in our analysis. Relative to this offset range, the maximum frequency separation of 3 x $^{1}J_{CH}$ between the multiplet components of the ^{13}C-methyl quartet is small, and therefore the difference between their saturation level is negligible. In addition, the amount of saturation is detected from one single cross peak per methyl group, yielding an averaged DEST effect even if the effect is slightly different for individual components of the multiplet.

The impact of cross-relaxation between ^{13}C nuclei, although larger than that between ^{15}N nuclei, is expected to be negligibly small. Relative to ^{1}H, given the same internuclear distances and dynamic properties (rotational correlation time, order parameters, etc….), the effect for ^{13}C is 256 times weaker than for ^{1}H. Because the dependence of this effect on internuclear distance is extremely steep (r^{-6}) and because spin diffusion is a second order effect, ^{13}C-^{13}C cross-relaxation may only become an issue when two ^{13}C nuclei are directly bonded to one another and if the two ^{13}C spins are saturated to very different levels. Therefore, the ^{13}C-^{13}C cross-relaxation effect, if significant, should have most impacted the DEST profiles obtained for Ala methyls due to the large chemical shift difference between Cα and methyl Cβ carbons. In practice, however, we did not observe asymmetry in the DEST profiles for Ala methyls that may be caused by this cross-relaxation effect.

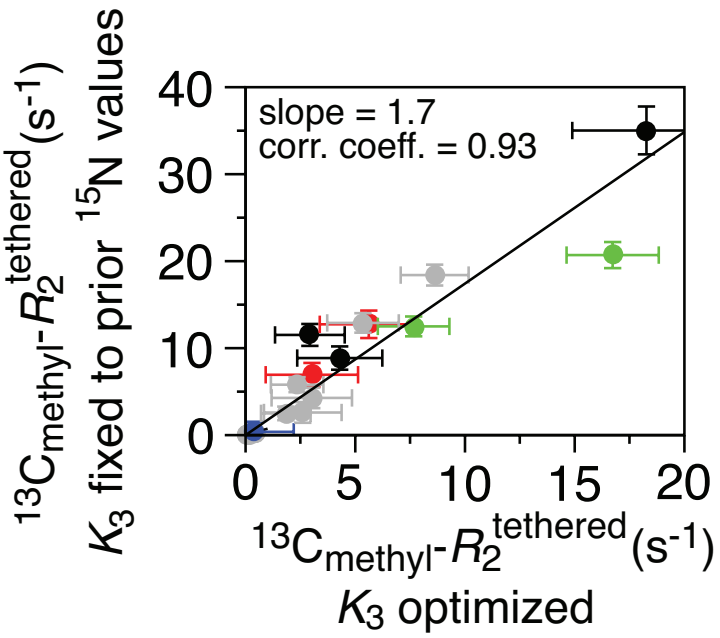

Figure S6. Correlation between optimized values of $^{13}C_{methyl}$-$R_2^{tethered}$ obtained from calculations in which the partition coefficient K_3 was either optimized (main text) or fixed to the values previously obtained from analysis of ^{15}N ΔR_2 and DEST data[S1]. Although the values of $^{13}C_{methyl}$-$R_2^{tethered}$ and $^{13}C_{methyl}$-$R_2^{contact}$ (1330±80 versus 2100±65 s^{-1}) obtained with K_3 optimized are systematically smaller, the conclusions in the main paper are not affected as the $^{13}C_{methyl}$-$R_2^{tethered}$ values obtained with and without K_3 optimization are highly correlated. The smaller values of $^{13}C_{methyl}$-$R_2^{tethered}$ obtained with K_3 optimization are associated with correspondingly larger values of the partition coefficient K_3 (see Figures 3A and 4B, main text). The optimized values of K_3, however, are still highly correlated with those obtained previously from the ^{15}N data (Figure 4B, main text), so again the conclusions are unaffected.

Supplementary references

[S1] N. L. Fawzi, J. Ying, R. Ghirlando, D. A. Torchia, G. M. Clore, *Nature* **2011**, *480*, 268-272.

[S2] T. Yamaguchi, K. Matsuzaki, M. Hoshinmo, *FEBS Lett* **2011**, 585, 1097-1102

[S3] L.E. Kay, T.E. Bull, L.K. Nicholson, C. Griesinger, H. Schwalbe, A. Bax, D.A. Torchia, *J. Magn. Reson.* **1992**, ***100***, 538-558.

[S4] H. Geen, R. Freeman, *J Am Chem Soc* **1991**, 9, 3596-3597.

[S5] A. J. Baldwin, L. E. Kay, *J Biomol NMR* **2012**, 53, 1-12.

[S6] L. K. Nicholson, L. E. Kay, D. M. Baldisseri, J. Arango, P. E. Young, A. Bax, D. A. Torchia, *Biochemistry* **1992**, 31, 5253-5263.